Studies of galactic sources with image restoration techniques

H. Tajima, A. Okumura (Nagoya Univ.), Y. Uchiyama (Rikkyo Univ.), T. Mizuno (Hiroshima Univ.), J. Cohen-Tanugi (IN2P3/CNRS)
on behalf of the Fermi Large Area Telescope Collaboration

Summary: We present an image restoration technique based on the Richardson-Lucy algorithm with an ability to properly incorporate point sources and known diffuse sources, which is useful for image analyses of galactic sources.

Introduction:

We have developed an image restoration technique based on the Richardson-Lucy algorithm[1] optimized for image analyses of *Fermi* Large Area Telescope (*Fermi*-LAT). This technique is unique since it takes advantage of the Point Spread Function (PSF) class of the Pass8 data set for each event, which is critical for *Fermi*-LAT image analysis since the PSF depends on the energy and angle of incident gamma rays and varies by more than one order of magnitude. *Fermi*-LAT image analysis also faces Poisson noise due to low photon statistics. Our technique incorporates wavelet filtering[2] to minimize such noise effects. In addition, this technique can utilize the diffuse background model as a part of the prior image so that we can produce an extended image of residual gamma rays. We present studies of galactic extended sources and point sources in the galactic center region using this image restoration technique.

Image Restoration Technique:

The observed image $\phi(x)$ is a convolution of the true image $\psi(\xi)$ and the instrument response function (IRF) $P(x|\xi)$, where $P(x|\xi)$ is the probability that the photon is observed at x when the true position is ξ. Based on a Bayesian approach, the original image $\psi(\xi)$ can be obtained iteratively:

$$\psi^{r+1}(\xi) = \frac{1}{N}\psi^{r}(\xi)\sum_{k=1}^{N}\frac{P_k(x_k|\xi)}{\int P_k(x_k|\zeta)\psi^{r}(\zeta)d\zeta},$$

where x_k and $P_k(x_k|\xi)$ is the observed position and IRF of the k^{th} photon. It is proven mathematically that $\psi^{r+1}(\xi)$ yields larger likelihood than $\psi^{r}(\xi)$ at each iteration. However, this algorithm suffers from the amplification of the noise (mostly Poisson noise due to poor statistics for *Fermi*-LAT) as the number of iterations is increased.

Wavelet denoising can be used to suppress the noise in the residual between the observed and expected image at each iteration[3]. The residual, $\rho^{r}(x)$, is defined as $\rho^{r}(x) \equiv \phi(x) - \phi^{r}(x)$, where $\phi^{r}(x)$ is the convolved image defined as:

$$\phi^{r}(x) \equiv \int \Pi(x|\zeta)\psi^{r}(\zeta)d\zeta, \quad \Pi(x|\zeta) = \frac{\sum_{k=1}^{N} P_k(x|\zeta)P_k(x_k|x)}{\sum_{k=1}^{N} P_k(x_k|x)}.$$

Here $\Pi(x|\zeta)$ is the weighted average of the instrument response at a given position x. The residual is decomposed into J wavelet scales as

$$\rho^{r}(x) = c_J(x) + \sum_{j=1}^{J} w_j(x),$$

where $c_J(x)$ is the last smoothed image and ω denotes each wavelet scale. The residual can be filtered based on its significance as:

$$\rho'^{r}(x) = c_J(x) + \sum_{j=1}^{J} M_j(x)w_j(x),$$

where $M_j(x)$ is 0 if the $\omega_j(x)$ is consistent with noise and 1 otherwise. We currently use the 99% Poisson probability as the consistency threshold. The filtered residual is incorporated in the iteration process using the filtered image, $\phi'^{r}(x) = \rho'^{r}(x) + \phi^{r}(x)$:

$$\psi^{r+1}(\xi) = \frac{1}{N}\psi^{r}(\xi)\sum_{k=1}^{N}\frac{P_k(x_k|\xi)\phi'^{r}(x_k)/\phi(x_k)}{\int P_k(xk|\zeta)\psi^{r}(\zeta)d\zeta}.$$

The generalized formulas described here are completely equivalent to the non-generalized versions if $P_k(x|\xi)$ is common for all photons.

When we have point sources in the field, the probability density function, $\psi^{r}(\xi)$, can be decomposed into two components[4]:

$$\psi^{r}(\xi) = \psi^{r}_{\rm PS}(\xi) + \psi^{r}_{\rm ES}(\xi),$$

where $\psi^{r}_{\rm PS}(\xi)$ represents a point source component (mostly zero apart from δ-functions at the positions of the point sources) while $\psi^{r}_{\rm ES}(\xi)$ represents a component for extended sources. Wavelet filtering is applied only to the extended-source component. This dual channel method can be used to incorporate sharp point sources while keeping the smooth diffuse component. This effectively works as point source subtraction without negative values in $\psi^{r}_{\rm ES}(\xi)$ (straight point source subtraction often results in negative values due to noise).

We have extended the dual channel method by adding a third component, $\psi^{r}_{\rm DM}(\xi)$, to represent the known diffuse model. In order to preserve the image of this component, only the normalization of this component is recalculated as

$$\psi'^{r}_{\rm DM}(\xi) = \frac{\int \psi^{r}_{\rm DM}(\xi)}{\int \psi^{0}_{\rm DM}(\xi)}\psi^{0}_{\rm DM}(\xi),$$

in each iteration.

References:

1. W. H. Richardson, Optical Society of America Jour. 62, 55 (1972). L. B. Lucy, Astron. Jour. 79, 745 (1974).
2. D. L. Donoho, IEEE Trans. on Infor. Theory 39 257 (1993).
3. J.-L. Starck and F. Murtagh, Astron. Astrophys. 288 342 (1994).
4. R. N. Hook and L. B. Lucy, "The Restoration of HST Images and Spectra," 1994.

Galactic Extended Source:

We have applied our technique to one of the extended gamma-ray sources in the galactic plane, RX J1713.7–3946. We have analyzed the *Fermi* data with $E > 10$ GeV for MET up to 493,448,876 (Aug 2016).

Top right figure shows the diffuse background model produced by a bilinear interpolation of gll_iem_v06.fits. Green contour represents the H.E.S.S. image of this source.

Bottom left figure shows the image that includes the diffuse background component, $\psi_{\rm ES}(\xi) + \psi_{\rm DM}(\xi)$, while bottom right figure shows the image that excludes the diffuse background, $\psi_{\rm ES}(\xi)$ only, which resembles the H.E.S.S. image. Most of artifacts in the galactic plane disappear and contrast of the extended source image is better without the diffuse background. The image also shows potential voids around (l,b) = (347.05, –0.3) and (347.65, –0.7) as indicated by white circles, compared with the H.E.S.S. image.

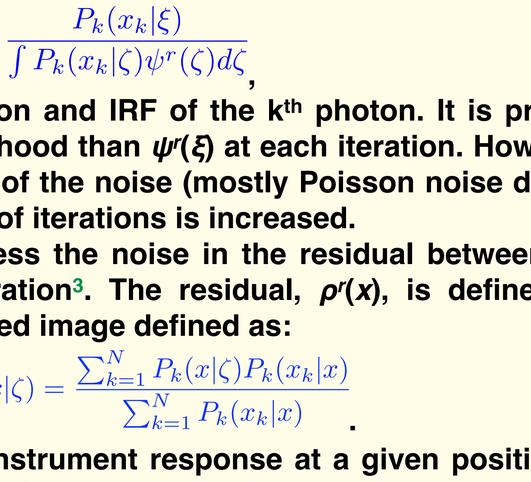

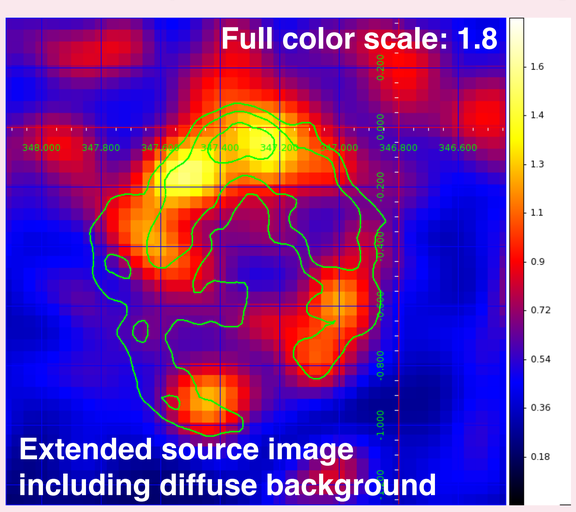

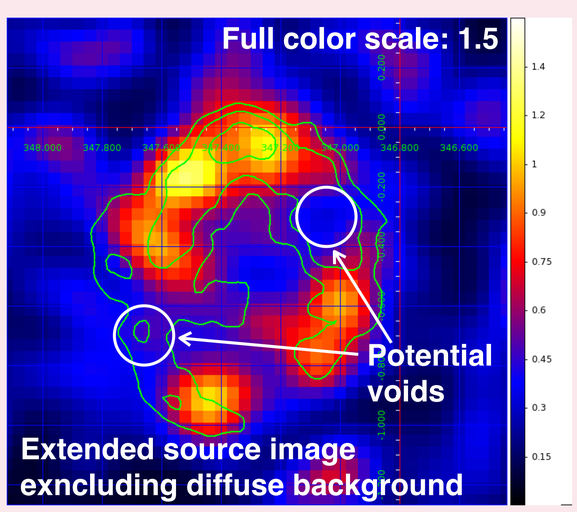

Point Source Analysis in Galactic Center Region:

We have also applied our technique to the galactic center region in an attempt to resolve undetected point sources. We have analyzed the *Fermi* data with PSF < 0.1° (68% containment) for MET up to 536,702,990 (Jan 2018).

Top right figure shows the count map smeared with PSF of each photon. Middle right figure shows the restored image excluding the diffuse background component and a very bright point source nearby the galactic center, J1745.6–2900, in log scale, where we utilized the diffuse background model developed for galactic center excess analysis by *Fermi*-LAT collaboration (2017ApJ...840...43A). Here we can clearly identify FL8Y sources, J1748.5–2814, J1747.2–2821, J1746.3–2852 and J1747.2–2958. We include those sources in the point source component, $\psi_{\rm PS}(\xi)$, and perform the image restoration again. The resulting image excluding the identified point sources and the diffuse background component is shown in bottom middle figure. Here, we can identify FL8Y sources, J1748.0–2825, J1748.1–2903 and J1746.5–2926. In addition, we identify potential unresolved sources, PS1: (266.54, –29.14), PS2: (265.90, –29.79) and PS3: (267.40, –28.89). After including these sources in the point source component, we obtain the image as shown in bottom right figure, where we may identify FL8Y J1746.5–3000. Remaining gamma-ray emission is still unresolved.